Alterations in the optic radiations of very preterm children—Perinatal predictors and relationships with visual outcomes ☆

Deanne K. Thompson [a,b,*], Dolly Thai [a], Claire E. Kelly [a], Alexander Leemans [c], Jacques-Donald Tournier [b], Michael J. Kean [d], Katherine J. Lee [a,e], Terrie E. Inder [f], Lex W. Doyle [a,g,h], Peter J. Anderson [a,e], Rodney W. Hunt [a,e,i]

[a] Murdoch Childrens Research Institute, Melbourne, Australia
[b] Florey Institute of Neuroscience and Mental Health, Melbourne, Australia
[c] Image Sciences Institute, University Medical Center Utrecht, The Netherlands
[d] Department of Medical Imaging, Royal Children's Hospital, Melbourne, Australia
[e] Department of Paediatrics, The University of Melbourne, Melbourne, Australia
[f] St. Louis Children's Hospital, Washington University in St. Louis, St. Louis, USA
[g] Royal Women's Hospital, Melbourne, Australia
[h] Department of Obstetrics and Gynaecology, The University of Melbourne, Australia
[i] Department of Neonatal Medicine, Royal Children's Hospital, Melbourne, Australia

ARTICLE INFO

ABSTRACT

Children born very preterm (VPT) are at risk for visual impairments, the main risk factors being retinopathy of prematurity and cerebral white matter injury, however these only partially account for visual impairments in VPT children. This study aimed to compare optic radiation microstructure and volume between VPT and term-born children, and to investigate associations between 1) perinatal variables and optic radiations; 2) optic radiations and visual function in VPT children. We hypothesized that optic radiation microstructure would be altered in VPT children, predicted by neonatal cerebral white matter abnormality and retinopathy of prematurity, and associated with visual impairments.

142 VPT children and 32 controls underwent diffusion-weighted magnetic resonance imaging at 7 years of age. Optic radiations were delineated using constrained spherical deconvolution tractography. Tract volume and average diffusion tensor values for the whole optic radiations and three sub-regions were compared between the VPT and control groups, and correlated with perinatal variables and 7-year visual outcome data.

Total tract volumes and average diffusion values were similar between VPT and control groups. On regional analysis of the optic radiation, mean and radial diffusivity were higher within the middle sub-regions in VPT compared with control children. Neonatal white matter abnormalities and retinopathy of prematurity were associated with optic radiation diffusion values. Lower fractional anisotropy in the anterior sub-regions was associated with poor visual acuity and increased likelihood of other visual defects.

This study presents evidence for microstructural alterations in the optic radiations of VPT children, which are largely predicted by white matter abnormality or severe retinopathy of prematurity, and may partially explain the higher rate of visual impairments in VPT children.

© 2013 The Authors. Published by Elsevier Inc. All rights reserved.

1. Introduction

Children born very preterm [VPT, <32 weeks' gestational age (GA)] are at high risk of visual impairments compared with children born at term (≥37 weeks' GA) (Arpino et al., 2010), which range from relatively subtle complications such as reduced visual acuity to complete blindness (Mirabella et al., 2006). Complex visual perceptual processes that rely on the integration of visual information are also often affected (Geldof et al., 2012). Such visual impairments may contribute to learning difficulties at school (Cooke et al., 2004). Major causes of visual impairment in VPT children include retinopathy of prematurity (ROP; pathologic vascular hyperproliferation in the immature retina (Palmer et al., 2005)) and overt cerebral white matter injury affecting the visual pathways (Ricci et al., 2006). However, visual impairments have been

* Corresponding author at: Victorian Infant Brain Studies (VIBeS), Murdoch Childrens Research Institute, Flemington Road Parkville, Victoria 3052, Australia. Tel.: +61 3 99366708.
E-mail address: deanne.thompson@mcri.edu.au (D.K. Thompson).

reported even in VPT children who have no history of ROP or overt cerebral injury (Kozeis et al., 2012), indicating that other factors may be associated with visual impairment in VPT children. By studying the white matter within the optic radiations, elucidation of potential neuro-anatomical correlates for visual impairment in VPT children may be possible.

One method that can be utilized to study the major tracts of the white matter is constrained spherical deconvolution (CSD) based tractography. CSD is an advanced diffusion-weighted magnetic resonance imaging (MRI) analysis method that is capable of modeling multiple fiber orientations, enabling robust delineation of white matter tracts (Tournier et al., 2007). Combined with the diffusion tensor model, non-invasive estimates of the microstructure and volume of specific white matter tracts can be made. Diffusion imaging has been applied to investigate the optic radiations in preterm infants in association with visual function assessed both in the neonatal period (Bassi et al., 2008; Berman et al., 2009; Groppo et al., 2012), and 6–20 months later (Glass et al., 2010). However, it is unknown whether further maturation and development of the optic radiations later into childhood strengthen or weaken relationships with visual function. The current study extends previous studies by investigating the association between optic radiation microstructure and volume and visual function at 7 years of age, when visual system structure and function is approaching full development (Birch and O'Connor, 2001). Furthermore, it associates optic radiations with neonatal MRI-detected white matter abnormality and ROP. It also extends previous studies by including a term-born control group, having access to a large sample size, and utilizing advanced CSD based tractography. The specific aims of the current study were to: 1) compare the microstructure and volume of the optic radiations between VPT children and controls at 7 years of age; 2) investigate relationships between perinatal variables and optic radiation structure in VPT children, particularly ROP and MRI-detected white matter abnormality; and 3) determine the relationship between optic radiation structure in VPT children and visual function assessed contemporaneously. It was hypothesized that: 1) optic radiation structure would be altered in VPT children compared with controls; 2) neonatal white matter abnormality and ROP would be associated with altered optic radiation structure in VPT children; and 3) altered optic radiation structure would be associated with visual impairments in VPT children.

2. Materials and methods

2.1. Participants

A prospective observational cohort of 227 children born <30 weeks' GA or <1250 g (which we will call the "VPT" group, acknowledging that it is different from the usual use of "VPT" as <32 weeks' GA) and 46 healthy term controls (born ≥ 37 weeks' GA) was recruited from the Royal Women's Hospital in Melbourne between July 2001 and December 2003. 2 VPT infants died and 1 was subsequently found to have a congenital abnormality, leaving 224 VPT children eligible. Children with congenital abnormalities or chromosomal disorders were also excluded. A total of 198 VPT children and 43 controls were followed-up at age 7 years. Of those who were followed-up, 160 VPT children and 36 controls underwent MRI, but 22 of these either did not have full diffusion datasets acquired or scans were unusable due to movement artifact. Thus the final number of children in the current study was 174 (64% of those recruited), including 142 VPT and 32 controls. Perinatal characteristics were similar between VPT participants who contributed optic radiation data and non-participants, with the exception of postnatal corticosteroid exposure (participants − 5.7%; non-participants −13.8%, p = 0.03).

The study was approved by the Royal Children's Hospital Human Research Ethics Committee and was performed in accordance with the ethical standards laid down in the 1964 Declaration of Helsinki and its later amendments. Informed consent was obtained from all parents/caregivers prior to inclusion in the study. Perinatal data were obtained by chart review at the time of hospital discharge.

2.2. Magnetic resonance imaging

At term-equivalent age, T_1 and T_2 weighted images were acquired on a 1.5 T scanner. Infants were immobilized in a vacuum fixation beanbag and scanned while sleeping, without sedation. A cerebral white matter abnormality score (range 0–17) was graded qualitatively, as previously described and validated (Kidokoro et al., 2013).

At 7 years of age, MRI was performed without anesthesia or sedation on a 3 T scanner. T_1 weighted three-dimensional rapid gradient-echo images were acquired: TR, 1900 ms; TE, 2.27 ms; matrix, 256 × 256; FOV, 210 × 210 mm; 0.8 mm³ isotropic voxels. Intracranial volumes were obtained from the T_1 weighted images using 'FreeSurfer' software (Buckner et al., 2004). Given that overall head size has been shown to influence white matter diffusion tensor values due to differential partial volume effects (Takao et al., 2011), intracranial volumes were used to control for partial volume effects or other white matter microstructural differences related to head size.

Two sets of echo-planar diffusion-weighted images were acquired; one with 25 non-collinear gradient directions and b-values ranging up to 1200 s/mm² (TR, 12000 ms; TE, 96 ms; matrix, 144 × 144; FOV, 250 × 250 mm; 1.7 mm³ isotropic voxels), and another with 45 gradient directions and a b-value of 3000 s/mm² (TR, 7400 ms; TE, 106 ms; matrix, 104 × 104; FOV, 240 × 240 mm; 2.3 mm³ isotropic voxels). The $b = 1200$ s/mm² data were processed using 'ExploreDTI' software (Leemans et al., 2009). Data were corrected for motion and eddy current induced distortions, incorporating re-orientation of the B-matrix. The diffusion tensor model was fitted, generating axial diffusivity (AD), radial diffusivity (RD), mean diffusivity (MD), and fractional anisotropy (FA) maps. CSD was applied to the $b = 3000$ s/mm² diffusion-weighted data using 'MRtrix' software (Tournier et al., 2012), creating a map of fiber orientation distributions in each voxel. A maximum harmonic order of 6 was used.

2.3. Fiber tractography

Probabilistic tractography was performed based on CSD's fiber orientation distributions. A seed region of interest was placed on an axial slice depicting the transition from the posterior limb of the internal capsule to the cerebral peduncle. The seed was positioned immediately lateral to the lateral geniculate nucleus within the white matter of the optic radiation at the apex of the arc around the lateral ventricles (Fig. 1A), as described previously (Ciccarelli et al., 2003). A target region of interest was positioned on a coronal slice encompassing the entire white matter cross-section of the optic radiation, just anterior to the primary visual cortex (Fig. 1B) (Berman et al., 2009). A maximum fiber orientation distribution amplitude of 0.2 was specified, and tracts were constrained to pass in one direction from the seed to target region of interest (Fig. 1C). Binary tract images were produced by counting the number of streamlines per voxels, and discarding voxels containing <6/1000 streamlines to reduce the likelihood of including aberrant fibers in the tract volume.

Diffusion metrics vary along the optic radiations due to variations in fiber density and geometry, partial volume effects and locations of injury (Berman et al., 2009; Yeatman et al., 2012). Therefore, the tracts were divided into three equal sub-regions by cutting the tracts one-third and two-thirds of the way from their most anterior to most posterior points (Fig. 1D, E and F).

Diffusion values (FA, RD, AD, MD) within the whole optic radiations and sub-regions were obtained by averaging values from the co-registered $b = 1200$ s/mm² diffusion tensor maps within the binary tract images. Diffusion values were obtained from the co-registered $b = 1200$ s/mm² maps rather than directly from the $b = 3000$ s/mm² maps because: 1) diffusion tensor values, particularly MD, vary according
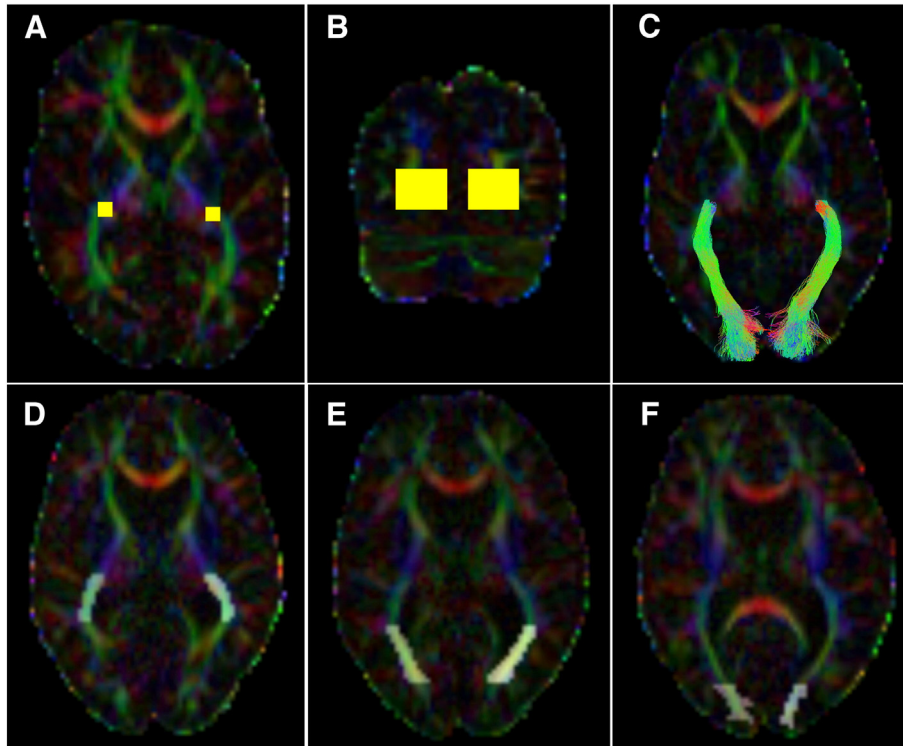
Fig. 1. Regions of interest for optic radiation tractography. (A) Seed regions of interest were defined on an axial slice and positioned immediately lateral to the lateral geniculate nuclei within the white matter of the optic radiations at the apex of the arc around the lateral ventricles. (B) Target regions of interest were placed on a coronal slice, designed to encompass the entire white matter cross-section of the optic radiations as they passed into the primary visual cortices. (C) Optic radiation white matter tracts of a very preterm 7-year-old. (D), (E), (F) Locations of the anterior, middle and posterior sub-regions of the optic radiations respectively.

to the strength and number of b-values in the acquisition (Melhem et al., 2000); 2) increasing b-values are accompanied by decreasing signal-to-noise ratios (Jones et al., 2012). As such, the $b = 1200$ s/mm^2 sequences may be expected to provide more accurate estimates of the diffusion tensor values than the $b = 3000$ s/mm^2 sequences. All co-registered images were visually examined for registration errors.

Intra-class correlation coefficients for tractography repeated on 20 randomly chosen participants were: tract volume $= 0.88$, FA $= 0.93$, AD $= 0.82$, RD $= 0.98$, MD $= 0.95$; indicating high intra-rater reliability by the single operator (D. Thai).

2.4. Visual function examination

Vision was assessed by a pediatrician masked to the clinical history of the children on the day of the 7-year MRI. Assessments were performed with the child's own (if any) corrective eyewear. Visual acuity was measured simultaneously for both eyes, using the standard Snellen eye chart, from a distance of 6 m. Results were recorded as Snellen decimals (Kniestedt and Stamper, 2003). Visual defects in either eye were recorded from previous opthalmological assessments and included strabismus, myopia, hypermetropia, cataracts, nystagmus, astigmatism, amblyopia or requirement for corrective lenses. Visual perception was assessed using the visual closure subtest from the Test of Visual Perceptual Skills − Third Edition (Martin, 2006), which requires children to identify whole figures from incomplete images. Relationships between visual closure score and measures from both the right and left optic radiations of VPT children were assessed separately, as the right hemisphere is considered dominant for visual closure (Wasserstein et al., 2004).

2.5. Statistical analysis

Data were analyzed using 'SPSS v20' (Chicago, IL). Exploratory analyses were initially performed to assess the distributions of optic radiation diffusion and volume data and visual outcomes for normality and outliers.

Baseline characteristics of the VPT and control groups that contributed 7-year optic radiation data were compared using t-tests, chi-squared tests or Mann–Whitney U tests, as appropriate.

Data from the whole optic radiations and sub-regions were compared between the VPT and control groups, with and without adjusting for age at MRI and intracranial volume, using linear regression.

Associations between clinically important perinatal variables and the optic radiation data of VPT children were investigated using multivariable linear regression: GA at birth; birth weight standard deviation score (BWSDS) (Cole et al., 1998); MRI-detected white matter abnormality score; female sex; severe ROP (maximum stage in either eye ≥ 3); postnatal corticosteroid exposure. Each perinatal variable was firstly entered into separate regression models. Secondly, all perinatal variables were entered simultaneously into the regression models, along with age at MRI and intracranial volume, to investigate the effect of each perinatal variable independent of the effects of the other perinatal variables, age at MRI and intracranial volume.

Within the VPT group, relationships were investigated between: 1) The optic radiation variables and visual acuity score using linear regression; 2) The optic radiation variables and the likelihood of visual defect of any kind in either eye using logistic regression; 3) The optic radiation variables and visual perception score using linear regression. These analyses were performed with and without adjusting for age at MRI, intracranial volume and the previously defined perinatal variables. Given that visual perception may be related to overall cognitive functioning, the third stage of analysis also excluded children with an intellectual impairment [full-scale IQ score < 70, as determined using the Wechsler Abbreviated Scale of Intelligence (WASI) (Wechsler, 1999)].

Given the multiple comparisons, the results were interpreted by considering overall patterns and magnitudes of differences, rather than by focusing on individual p-values.

Table 1
Perinatal characteristics and 7-year visual outcomes of the very preterm (VPT) and control cohorts.

Perinatal characteristics	VPT, n = 142	Controls, n = 32		
			Mean difference (95%CI)	p
GA at birth (weeks), mean (SD)	27.5 (1.9)	38.8 (1.3)	−11.3 (−12.0, −10.6)	<0.001
Birth weight (g), mean (SD)	972 (226)	3220 (489)	−2247 (−2360, −2135)	<0.001
BWSDS[a], mean (SD)	−0.51 (0.92)	−0.02 (0.92)	−0.49 (−0.85, −0.14)	0.007
			Odds ratio (95% CI)	p
Male, n (%)	70 (49.3)	15 (46.9)	0.9 (0.4, 2.0)	0.81
Postnatal corticosteroid therapy[b], n (%)	8 (5.7)[c]	0 (0)	*	0.17
Maximum stage ROP ≥ 3, either eye, n (%)	30 (24.4)[d]	0 (0)	*	0.002
Intraventricular hemorrhage grade III/IV, n (%)	5 (3.5)	0 (0)	*	0.28
Cystic periventricular leukomalacia, n (%)	5 (3.5)	0 (0)	*	0.28
			Z value	p
White matter abnormality score, median (25th–75th percentile)	3 (1–4)	1 (0–2)	−5.03	<0.001
7-year characteristics				p
			Mean difference (95%CI)	p
Age at imaging (years), mean (SD)	7.5 (0.2)	7.6 (0.2)	−0.08 (−0.17, 0.02)	0.11
Full-scale IQ score, mean (SD)	98.8 (12.8)	109.6 (11.5)	−10.8 (−15.6, −5.9)	<0.001
Total intracranial volume (cm³), mean (SD)	1331.3 (121.8)[c]	1421.8 (104.8)	−90.5 (−136.5, −44.5)	<0.001
Total white matter volume (cm³), mean (SD)	403.6 (46.8)[e]	444.6 (42.9)[f]	−41.1 (−59.6, −22.6)	<0.001
Visual acuity, mean (SD)	0.99 (0.21)[g]	1.12 (0.22)[f]	−0.13 (−0.22, −0.05)	0.002
Visual closure total raw score, mean (SD)	5.2 (3.1)[c]	7.3 (3.1)[h]	−2.1 (−3.3, −0.9)	0.001
			Odds ratio (95% CI)	p
Visual defect of any kind in either eye, n (%)	33 (23.6)[i]	4 (12.5)	2.2 (0.7, 6.6)	0.17
Strabismus, n (%)	0 (0)	0 (0)	*	*
Astigmatism, n (%)	9 (6.3)	2 (6.3)	1.0 (0.2, 4.9)	0.99
Myopia, n (%)	8 (5.6)	2 (6.3)	0.9 (0.2, 4.4)	0.89
Amblyopia, n (%)	1 (0.7)	1 (3.1)	0.2 (0.01, 3.6)	0.25
Hypermetropia, n (%)	5 (3.5)	1 (3.1)	1.1 (0.1, 10.0)	0.91
Cataract, n (%)	0 (0)	0 (0)	*	*
Nystagmus, n (%)	0 (0)	0 (0)	*	*
Corrective lenses prescribed, n (%)	9 (6.3)	1 (3.1)	2.1 (0.3, 17.2)	0.48

BWSDS = birth weight standard deviation score, CI = confidence interval, GA = gestational age, ROP = retinopathy of prematurity, SD = standard deviation. * Indicates not possible to calculate as there is a zero value in one or more cells.
[a] BWSDS computed relative to the British Growth Reference data (Cole et al., 1998).
[b] Postnatal dexamethasone, usual dose 0.15 mg/kg per day for 3 days, reducing over 10 days: total dose 0.89 mg/kg.
[c] n = 141.
[d] n = 123.
[e] n = 124.
[f] n = 30.
[g] n = 133.
[h] n = 31.
[i] n = 140.

3. Results

Table 1 reports sample characteristics of the 142 VPT children and 32 controls with optic radiation data at age 7 years. Age at the 7-year MRI and the proportion of males was similar between the VPT and control groups, but many other perinatal characteristics differed as expected. Of note, intracranial volume was lower in the VPT children, and the VPT group exhibited poorer visual acuity and visual perception (visual closure).

3.1. Very preterm children vs. controls

There was higher diffusivity within the optic radiations of the VPT children than controls, particularly in the middle sub-region, even after adjusting for age at MRI and intracranial volume (Fig. 2A). There was evidence that optic radiation volume was smaller in the VPT children compared with the controls in the posterior sub-region in an unadjusted analysis [mean difference (95% confidence interval (CI)) = −0.4 (−0.8, −0.04) cm³, p = 0.03], although this group difference was less marked after adjustment for age at MRI and intracranial volume (Fig. 2B).

3.2. Perinatal predictors

Within VPT children, higher neonatal white matter abnormality scores were associated with higher AD, RD and MD in the optic radiations, particularly in the middle sub-region. Higher neonatal white matter abnormality scores were also associated with lower optic radiation FA

in VPT children, both overall and in the anterior and middle sub-regions (Fig. 3). These associations remained after adjusting for age at MRI, intracranial volume and the remaining perinatal variables (data not shown). There was also evidence that severe ROP was associated with higher AD, RD and MD in VPT children, particularly in the middle sub-region (Fig. 3); adjustment for age at MRI, intracranial volume and the remaining perinatal variables had little effect (data not shown). There was little evidence of associations between GA at birth, BWSDS, sex or postnatal corticosteroid exposure and optic radiation diffusion values in VPT children (Fig. 3).

Female sex was associated with lower optic radiation volume in VPT children, particularly in the posterior sub-region (Fig. 3E); adjustment for age at MRI, intracranial volume and the remaining perinatal variables had little effect (data not shown). There was little evidence of associations between GA at birth, BWSDS, postnatal corticosteroid exposure, neonatal white matter abnormality or severe ROP and optic radiation volume in VPT children (Fig. 3E).

3.3. Visual outcome

Within the VPT group there was little evidence of associations between optic radiation diffusion values and visual acuity, except higher FA in the anterior sub-region was associated with higher (better) visual acuity scores. This association remained after adjusting for age at MRI, intracranial volume and the previously defined perinatal variables (Fig. 4A). Increased optic radiation volume was associated with better
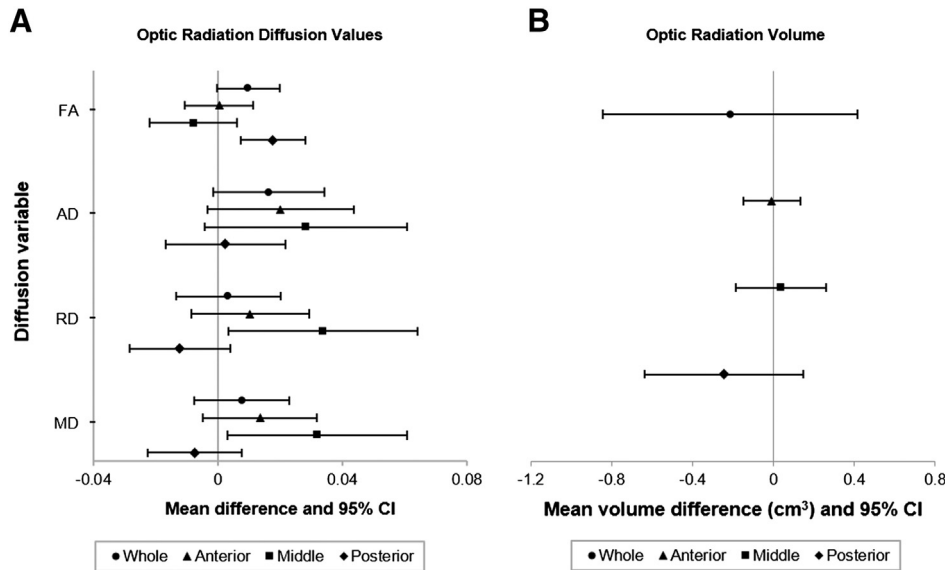
Fig. 2. Mean differences in optic radiation variables [(A) diffusion values within the optic radiations, (B) optic radiation volume] in very preterm (VPT) compared with term-born control children. Results presented are adjusted for age at MRI and intracranial volume. AD = axial diffusivity ($\times 10^{-3}$ mm^2/s), CI = confidence interval, FA = fractional anisotropy, MD = mean diffusivity ($\times 10^{-3}$ mm^2/s), RD = radial diffusivity ($\times 10^{-3}$ mm^2/s).

visual acuity for all regions, with similar results after adjusting for age at MRI, intracranial volume and perinatal variables (Fig. 4B).

Reduced optic radiation FA both overall and within the anterior and middle sub-regions, of VPT children was associated with increased odds of visual defect in either eye, a finding that remained after adjustment for age at MRI, intracranial volume and perinatal variables (Fig. 5A). There was also some suggestion that increased RD was associated with increased odds of a visual defect. There was little evidence of associations between optic radiation volume and visual defect in VPT children (Fig. 5B).

There was some suggestion that lower RD and MD, particularly in the anterior sub-region, of both the left and right optic radiations of VPT children was associated with higher (better) visual closure scores, with some attenuation of these associations after adjusting for age at MRI, intracranial volume and perinatal variables (Fig. 6A and B). There was little evidence of associations between right or left optic radiation volume and visual closure in VPT children (Fig. 6C). These findings were similar when the only child with a full-scale IQ score <70 was excluded (data not shown).

4. Discussion

In summary, optic radiation diffusivity, particularly in the middle sub-region, was higher in the VPT children than controls. Neonatal white matter abnormality and severe ROP were associated with higher diffusivity within the optic radiations of VPT children, particularly within the middle sub-region. Female sex was also associated with lower optic radiation volume in VPT children. Furthermore, in VPT children increasing optic radiation FA, particularly in the anterior sub-region, was associated with better visual acuity and decreased likelihood of other visual defects.

Diffusivity was higher in the optic radiations in the VPT group compared with controls. This finding suggests that the microstructure of the optic radiations is altered in VPT children compared with controls. Such changes in VPT children may reflect changes in white matter fiber diameter or density, myelination or membrane permeability (Jones et al., 2012). The findings may also suggest that optic radiation development is altered in VPT children compared with term-born children, which is supported by previous studies reporting that in typically developing children AD, RD and MD decrease over time in the white matter (Mukherjee and McKinstry, 2006). The detection of diffusion differences

between VPT children and controls in the middle sub-region to a greater extent than in the anterior and posterior sub-regions may relate to variations in axonal architecture along the tracts, or localization of injuries at specific points along the tracts (Berman et al., 2009; Yeatman et al., 2012). Additionally, there may be reduced influence by confounding factors such as crossing fibers in the middle sub-region, giving greater sensitivity to find group-wise differences. Optic radiation volumes, particularly in the posterior sub-region, appeared smaller in the VPT children. However, this finding was largely explained by reduced intracranial volume and/or confounding from age at MRI. This finding is consistent with Gimenez et al., who found little difference in optic radiation volume between VPT and control adolescents (Gimenez et al., 2006).

Within the VPT group, higher MRI-detected neonatal white matter abnormality scores predicted increased diffusivity and reduced FA in the whole optic radiations, and particularly the middle sub-region. This suggests that optic radiation microstructure is particularly altered in VPT children who had higher white matter abnormality scores in the newborn period. Similarly, there have been previous reports indicating that early white matter abnormalities correlate strongly with altered white matter diffusion tensor values in preterm children and adolescents, including lower FA and higher AD, RD and MD (Bonifacio et al., 2010; Feldman et al., 2012).

VPT children with severe ROP in infancy displayed higher diffusivity, particularly in the middle sub-region, than VPT children with no or mild ROP (<stage 3), suggesting an association between severe ROP and altered optic radiation microstructure. It is possible that visual deprivation from the ROP-affected eye may directly affect visual pathway development. Supporting this, reduced optic nerve fiber thickness was recently found in preterm children with severe ROP compared with term controls (Akerblom et al., 2012). Relationships between severe ROP and altered optic radiation microstructure may also reflect association with a common etiological factor, such as hypoxic–ischemic insult, which has been implicated in the causal pathways to both ROP (Stout and Stout, 2003) and cerebral white matter injury (Volpe, 2009). In contrast to our findings, Bassi et al. reported similar optic radiation diffusion tensor values between preterm infants with and without ROP at term equivalent age (Bassi et al., 2008). However, Bassi et al.'s study included only 8 infants with mild ROP (stage 1 or 2) that had resolved by the time of MRI. In the current study, 30 VPT children had severe ROP (≥stage 3)
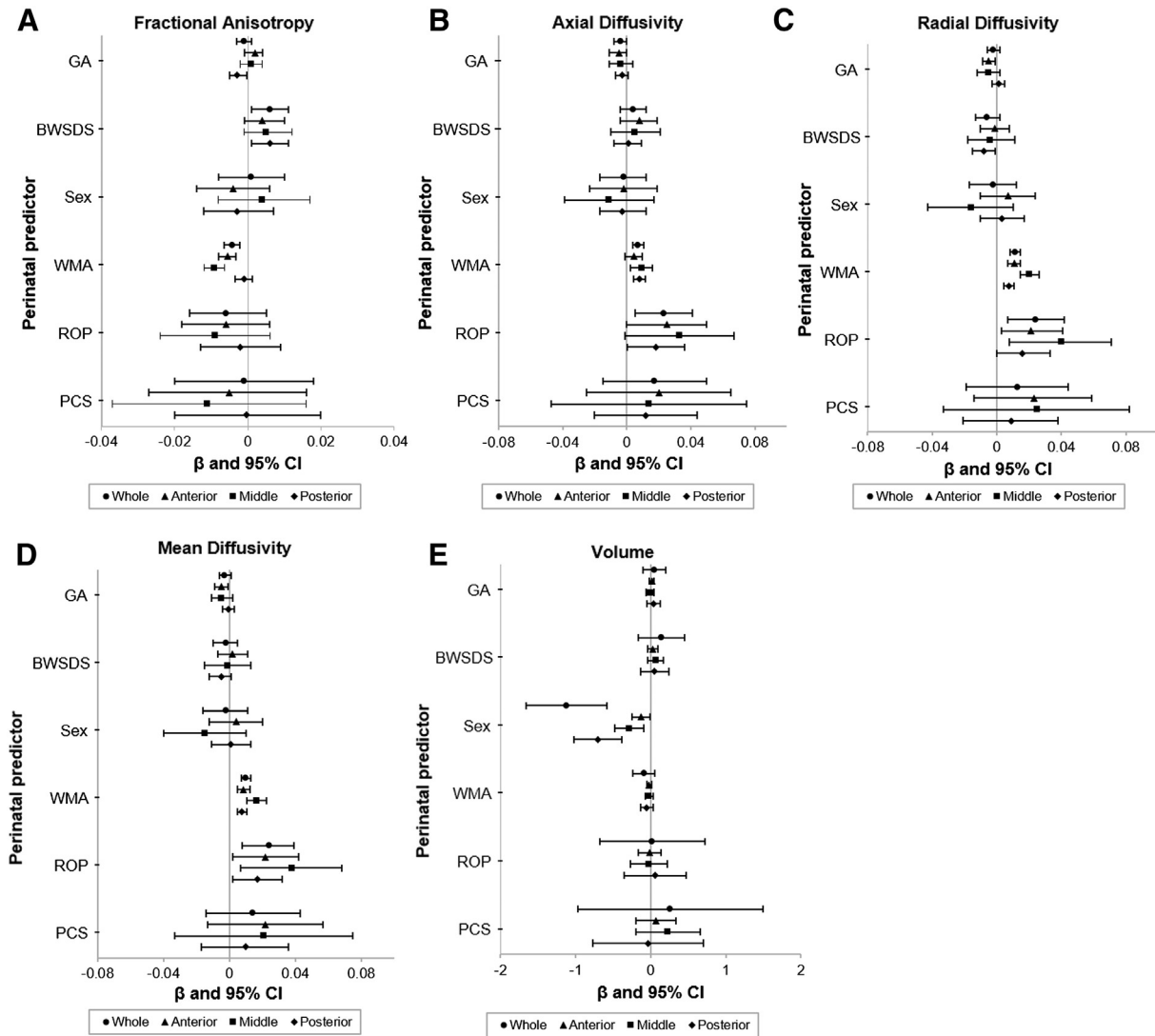
Fig. 3. Relationships between perinatal variables and optic radiation variables in the VPT children [(A) fractional anisotropy, (B) axial diffusivity, (C) radial diffusivity, (D) mean diffusivity and (E) tract volume]. Results presented are regression coefficients, representing the difference in optic radiation per unit change in the predictor, from an unadjusted analysis. AD = axial diffusivity ($\times 10^{-3}$ mm²/s), BWSDS = birth weight standard deviation score, CI = confidence interval, FA = fractional anisotropy, GA = gestational age at birth (weeks), MD = mean diffusivity ($\times 10^{-3}$ mm²/s), PCS = postnatal corticosteroid exposure, RD = radial diffusivity ($\times 10^{-3}$ mm²/s), ROP = severe retinopathy of prematurity, WMA = white matter abnormality score, β = regression coefficient.

in infancy, enabling detection of microstructural differences between VPT children who had no or mild ROP and those with severe ROP in infancy.

Female sex was associated with lower optic radiation volume in VPT children, particularly in the posterior sub-region, even after adjustment for intracranial volume, age at MRI and the remaining tested perinatal variables. A possible explanation is that relative white matter volume increases more rapidly in males than females throughout childhood and adolescence, particularly in the frontal and occipital regions (Lenroot et al., 2007).

In the VPT children, increasing FA in the anterior optic radiation sub-region was associated with better visual acuity and decreased likelihood of other visual defects. Similarly, previous work has reported correlations between diffusion values within the optic radiations of preterm *neonates* and functional visual outcome (Bassi et al., 2008; Berman et al., 2009; Glass et al., 2010). Together, these findings may suggest that structure–function relationships exist between optic radiation diffusion values and visual functions relying on visual cortical processing. The current study suggests that relationships between optic radiation structure and visual function in VPT children persist beyond infancy, and up to 7 years of age.

There was evidence of associations between RD and MD in both the right *and* left optic radiations of VPT children and our measure of visual perception (visual closure). However these associations may have been explained by age at MRI, intracranial volume and/or the previously defined perinatal variables. Additionally, similar patterns of associations were observed for the right and left optic radiations, despite reports that the right visual cortex is dominant for visual closure (Wasserstein et al., 2004). Right and left optic radiation diffusion values are highly correlated, therefore an association between microstructure and visual closure in one hemisphere is likely to be present in the other.

A limitation of this study was that a proportion of children in the cohort did not have useable diffusion-weighted images. Furthermore, the participants in this analysis tended to be healthier, with a smaller proportion of VPT participants exposed to postnatal corticosteroids compared with non-participants, and our findings may have been stronger if the entire cohort had been able to be assessed with MRI at 7 years of age.

There are limitations associated with using Snellen charts to measure visual acuity. Particularly in patients with low vision, the accuracy of Snellen acuity recordings may be affected by chart features such as non-uniform changes in letter sizes from line to line, variations in the
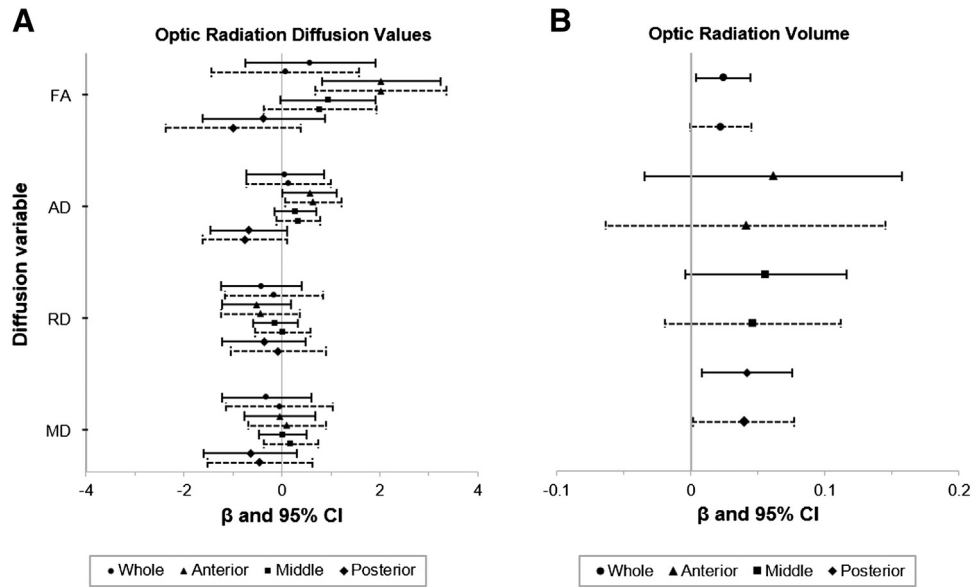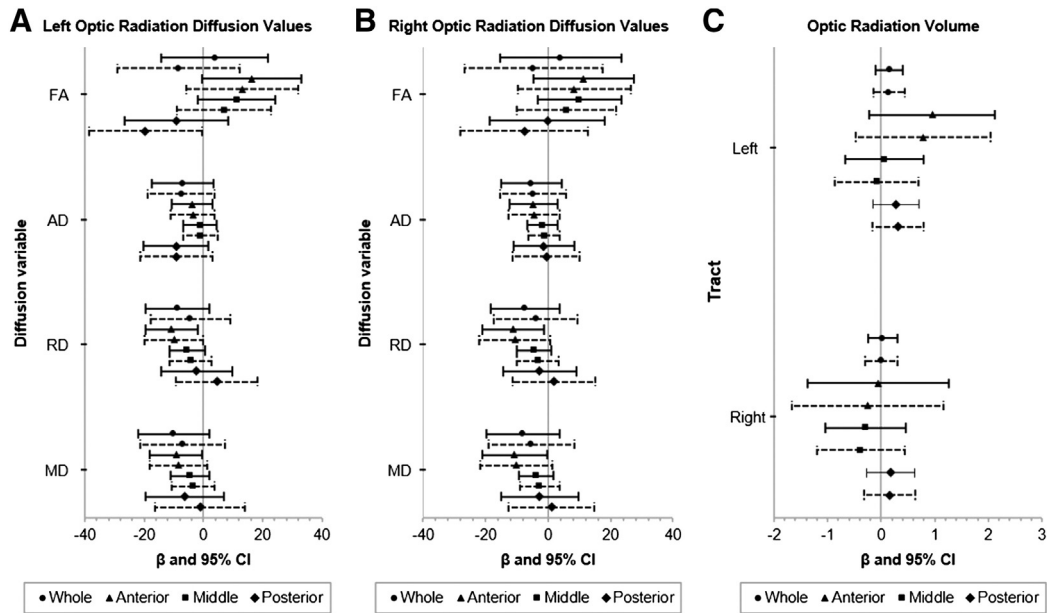
Fig. 4. Relationships between optic radiation variables [(A) diffusion values within the optic radiations, (B) optic radiation volume] and visual acuity score in VPT children. Solid lines represent regression coefficients from an unadjusted analysis and broken lines represent regression coefficients adjusted for age at MRI, intracranial volume and clinically important perinatal variables (gestational age at birth, birth weight standard deviation score, sex, white matter abnormality score, severe retinopathy of prematurity and postnatal corticosteroid exposure). AD = axial diffusivity ($\times 10^{-3}$ mm^2/s), CI = confidence interval, FA = fractional anisotropy, MD = mean diffusivity ($\times 10^{-3}$ mm^2/s), RD = radial diffusivity ($\times 10^{-3}$ mm^2/s). β = regression coefficient.

numbers of letters per line, and inconsistencies in the spacing between letters and lines. These and other disadvantages of Snellen charts have been discussed in detail previously (Kaiser, 2009; Kniestedt and Stamper, 2003). The accuracy with which visual acuity is measured may be improved in future studies by using, for example, Early Treatment Diabetic Retinopathy Study (ETDRS) charts rather than Snellen charts. Future studies may also benefit from assessing a wider range of visual functions, including stereopsis, contrast sensitivity and visual fields, in order to provide a more holistic view of visual system functioning in VPT children and the potential role of the optic radiations.

There are also limitations in using diffusion tensor measures to study the white matter. The tensor model enables detection of changes in several microstructural properties of the white matter (e.g. fiber density, myelination, etc.), but cannot sensitively distinguish between such factors. Moreover, diffusion tensor values may be influenced by the intra-voxel orientational coherence of fibers and by partial volume effects from non-white matter tissues (Jones et al., 2012). Recent work has demonstrated that FA (Alexander et al., 2001) and MD (Vos et al., 2012) are lower in crossing than single fiber regions, and that RD and AD may also be affected (Wheeler-Kingshott and Cercignani, 2009).
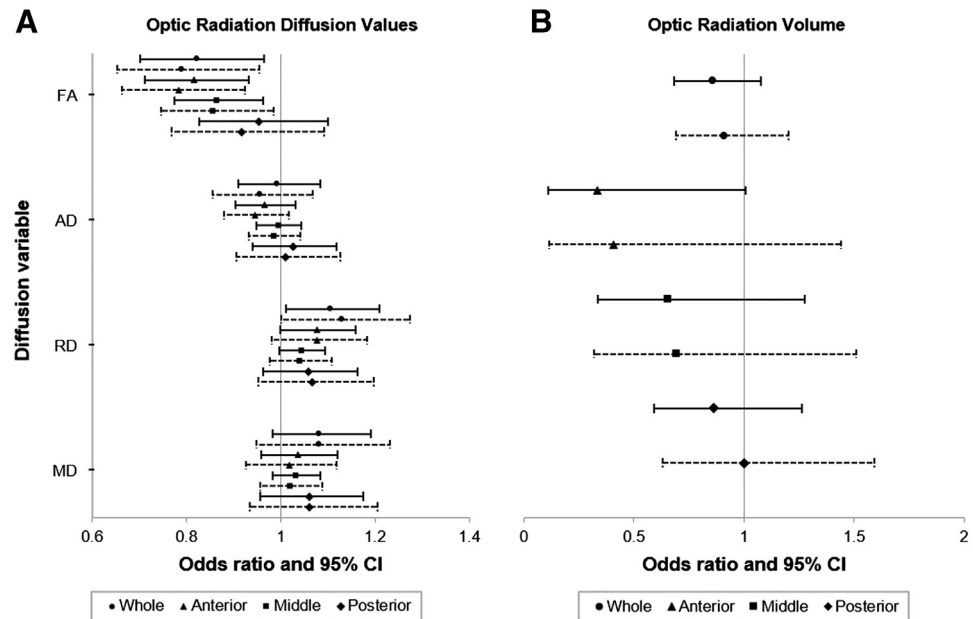
Fig. 5. Relationships between optic radiation variables [(A) diffusion values within the optic radiations, (B) optic radiation volume] and risk of visual defect in VPT children. Solid lines represent regression coefficients from an unadjusted analysis and broken lines represent regression coefficients adjusted for age at MRI, intracranial volume and clinically important perinatal variables (gestational age at birth, birth weight standard deviation score, sex, white matter abnormality score, severe retinopathy of prematurity and postnatal corticosteroid exposure). AD = axial diffusivity ($\times 10^{-3}$ mm^2/s), CI = confidence interval, FA = fractional anisotropy, MD = mean diffusivity ($\times 10^{-3}$ mm^2/s), RD = radial diffusivity ($\times 10^{-3}$ mm^2/s), β = regression coefficient.

Fig. 6. Relationships between optic radiation variables [(A) diffusion values within the left optic radiation, (B) diffusion values within the right optic radiation, (C) optic radiation volume], and visual closure scores in VPT children. Solid lines represent regression coefficients from an unadjusted analysis and broken lines represent regression coefficients adjusted for age at MRI, intracranial volume and clinically important perinatal variables (gestational age at birth, birth weight standard deviation score, sex, white matter abnormality score, severe retinopathy of prematurity and postnatal corticosteroid exposure). AD = axial diffusivity ($\times 10^{-3}$ mm^2/s), CI = confidence interval, FA = fractional anisotropy, MD = mean diffusivity ($\times 10^{-3}$ mm^2/s), RD = radial diffusivity ($\times 10^{-3}$ mm^2/s), β = regression coefficient.

Future work may use the recently developed 'Apparent Fibre Density' (Raffelt et al., 2012), which is based on CSD's fiber orientation distributions, to improve interpretation of diffusion changes in crossing fiber regions.

Tract thickness, orientation and curvature may also affect the diffusion tensor measures, in part by influencing the extent of partial volume effects (Vos et al., 2011). The current study attempted to control for partial volume effects by adjusting for intracranial volume in statistical analyses. Along with intracranial volume, other measures and methods have been proposed to control for partial volume effects, such as total white matter volume or regional tract volume, and there is some uncertainty as to which is most appropriate (Metzler-Baddeley et al., 2012).

Additionally, despite using CSD tractography to obtain robust tract delineations (Tournier et al., 2007), this study was unable to consistently track Meyer's loop.

5. Conclusions

VPT birth is associated with altered optic radiation microstructure in childhood, particularly within the middle sub-region, relative to birth at term. Such microstructural alterations in VPT children may be predicted by complications resulting from VPT birth such as MRI-detected white matter abnormalities and severe ROP. Moreover, altered optic radiation microstructure in VPT children, particularly in the anterior sub-region, is associated with reduced visual acuity and increased likelihood of other visual defects. These findings may partially explain the high rates of visual impairments in VPT children. By further elucidating the neural correlates of visual impairments in VPT children, the current findings may ultimately aid in improving the functional visual outcome of VPT children.

Acknowledgments

References

Akerblom, H., Holmstrom, G., Eriksson, U., Larsson, E., 2012. Retinal nerve fibre layer thickness in school-aged prematurely-born children compared to children born at term. Br. J. Ophthalmol. 96, 956–960.

Alexander, A.L., Hasan, K.M., Lazar, M., Tsuruda, J.S., Parker, D.L., 2001. Analysis of partial volume effects in diffusion-tensor MRI. Magn. Reson. Med. 45, 770–780.

Arpino, C., Compagnone, E., Montanaro, M.L., Cacciatore, D., De Luca, A., Cerulli, A., Di Girolamo, S., Curatolo, P., 2010. Preterm birth and neurodevelopmental outcome: a review. Childs Nerv. Syst. 26, 1139–1149.

Bassi, L., Ricci, D., Volzone, A., Allsop, J.M., Srinivasan, L., Pai, A., Ribes, C., Ramenghi, L.A., Mercuri, E., Mosca, F., Edwards, A.D., Cowan, F.M., Rutherford, M.A., Counsell, S.J., 2008. Probabilistic diffusion tractography of the optic radiations and visual function in preterm infants at term equivalent age. Brain 131, 573–582.

Berman, J.I., Glass, H.C., Miller, S.P., Mukherjee, P., Ferriero, D.M., Barkovich, A.J., Vigneron, D.B., Henry, R.G., 2009. Quantitative fiber tracking analysis of the optic radiation correlated with visual performance in premature newborns. Am. J. Neuroradiol. 30, 120–124.

Birch, E.E., O'Connor, A.R., 2001. Preterm birth and visual development. Semin. Neonatol. 6, 487–497.

Bonifacio, S.L., Glass, H.C., Chau, V., Berman, J.I., Xu, D., Brant, R., Barkovich, A.J., Poskitt, K.J., Miller, S.P., Ferriero, D.M., 2010. Extreme premature birth is not associated with impaired development of brain microstructure. J. Pediatr. 157 (726–732), e721.

Buckner, R.L., Head, D., Parker, J., Fotenos, A.F., Marcus, D., Morris, J.C., Snyder, A.Z., 2004. A unified approach for morphometric and functional data analysis in young, old, and demented adults using automated atlas-based head size normalization: reliability and validation against manual measurement of total intracranial volume. NeuroImage 23, 724–738.

Ciccarelli, O., Parker, G.J., Toosy, A.T., Wheeler-Kingshott, C.A., Barker, G.J., Boulby, P.A., Miller, D.H., Thompson, A.J., 2003. From diffusion tractography to quantitative white matter tract measures: a reproducibility study. NeuroImage 18, 348–359.

Cole, T.J., Freeman, J.V., Preece, M.A., 1998. British 1990 growth reference centiles for weight, height, body mass index and head circumference fitted by maximum penalized likelihood. Stat. Med. 17, 407–429.

Cooke, R.W., Foulder-Hughes, L., Newsham, D., Clarke, D., 2004. Ophthalmic impairment at 7 years of age in children born very preterm. Arch. Dis. Child. Fetal Neonatal Ed. 89, F249–F253.

Feldman, H.M., Lee, E.S., Loe, I.M., Yeom, K.W., Grill-Spector, K., Luna, B., 2012. White matter microstructure on diffusion tensor imaging is associated with conventional magnetic resonance imaging findings and cognitive function in adolescents born preterm. Dev. Med. Child Neurol. 54, 809–814.

Geldof, C.J., van Wassenaer, A.G., de Kieviet, J.F., Kok, J.H., Oosterlaan, J., 2012. Visual perception and visual-motor integration in very preterm and/or very low birth weight children: a meta-analysis. Res. Dev. Disabil. 33, 726–736.

Gimenez, M., Junque, C., Narberhaus, A., Bargallo, N., Botet, F., Mercader, J.M., 2006. White matter volume and concentration reductions in adolescents with history of very preterm birth: a voxel-based morphometry study. NeuroImage 32, 1485–1498.

Glass, H.C., Berman, J.I., Norcia, A.M., Rogers, E.E., Henry, R.G., Hou, C., Barkovich, A.J., Good, W.V., 2010. Quantitative fiber tracking of the optic radiation is correlated with visual-evoked potential amplitude in preterm infants. Am. J. Neuroradiol. 31, 1424–1429.

Groppo, M., Ricci, D., Bassi, L., Merchant, N., Doria, V., Arichi, T., Allsop, J.M., Ramenghi, L., Fox, M.J., Cowan, F.M., Counsell, S.J., Edwards, A.D., Groppo, M., Ricci, D., Bassi, L, Merchant, N., Doria, V., Arichi, T., Allsop, J.M., Ramenghi, L., Fox, M.J., Cowan, F.M., Counsell, S.J., Edwards, A.D., 2012. Development of the optic radiations and visual function after premature birth. Cortex. http://dx.doi.org/10.1016/j.cortex.2012.02.008.

Jones, D.K., Knosche, T.R., Turner, R., 2012. White matter integrity, fiber count, and other fallacies: the do's and don'ts of diffusion MRI. NeuroImage 73, 239–254.

Kaiser, P.K., 2009. Prospective evaluation of visual acuity assessment: a comparison of snellen versus ETDRS charts in clinical practice (an AOS thesis). Trans. Am. Ophthalmol. Soc. 107, 311–324.

Kidokoro, H., Neil, J., Inder, T.E., 2013. A new MRI assessment tool to define brain abnormalities in very preterm infants at term. Am. J. Neuroradiol. http://dx.doi.org/10.3174/ajnr.A3521.

Kniestedt, C., Stamper, R.L., 2003. Visual acuity and its measurement. Ophthalmol. Clin. North Am. 16 (155–170), v.

Kozeis, N., Mavromichali, M., Soubasi-Griva, V., Agakidou, E., Zafiriou, D., Drossou, V., 2012. Visual function in preterm infants without major retinopathy of prematurity or neurological complications. Am. J. Perinatol. 29, 747–754.

Leemans, A., Jeurissen, B., Sijbers, J., Jones, D.K., 2009. ExploreDTI: a graphical toolbox for processing, analyzing, and visualizing diffusion MR data. 17th Annual Meeting of Intl Soc Mag Reson Med, Hawaii, USA, p. 3537.

Lenroot, R.K., Gogtay, N., Greenstein, D.K., Wells, E.M., Wallace, G.L., Clasen, L.S., Blumenthal, J.D., Lerch, J., Zijdenbos, A.P., Evans, A.C., Thompson, P.M., Giedd, J.N., 2007. Sexual dimorphism of brain developmental trajectories during childhood and adolescence. NeuroImage 36, 1065–1073.

Martin, N., 2006. Test of Visual Perceptual Skills, Third Edition (TVPS-3). Academic Therapy Publications, Novato, California.

Melhem, E.R., Itoh, R., Jones, L., Barker, P.B., 2000. Diffusion tensor MR imaging of the brain: effect of diffusion weighting on trace and anisotropy measurements. AJNR Am. J. Neuroradiol. 21, 1813–1820.

Metzler-Baddeley, C., O'Sullivan, M.J., Bells, S., Pasternak, O., Jones, D.K., 2012. How and how not to correct for CSF-contamination in diffusion MRI. NeuroImage 59, 1394–1403.

Mirabella, G., Kjaer, P.K., Norcia, A.M., Good, W.V., Madan, A., 2006. Visual development in very low birth weight infants. Pediatr. Res. 60, 435–439.

Mukherjee, P., McKinstry, R.C., 2006. Diffusion tensor imaging and tractography of human brain development. Neuroimaging Clin. N. Am. 16 (19–43), vii.

Palmer, E.A., Hardy, R.J., Dobson, V., Phelps, D.L., Quinn, G.E., Summers, C.G., Krom, C.P., Tung, B., 2005. 15-year outcomes following threshold retinopathy of prematurity: final results from the multicenter trial of cryotherapy for retinopathy of prematurity. Arch. Ophthalmol. 123, 311–318.

Raffelt, D., Tournier, J.D., Rose, S., Ridgway, G.R., Henderson, R., Crozier, S., Salvado, O., Connelly, A., 2012. Apparent fibre density: a novel measure for the analysis of diffusion-weighted magnetic resonance images. NeuroImage 59, 3976–3994.

Ricci, D., Anker, S., Cowan, F., Pane, M., Gallini, F., Luciano, R., Donvito, V., Baranello, G., Cesarini, L., Bianco, F., Rutherford, M., Romagnoli, C., Atkinson, J., Braddick, O., Guzzetta, F., Mercuri, E., 2006. Thalamic atrophy in infants with PVL and cerebral visual impairment. Early Hum. Dev. 82, 591–595.

Stout, A.U., Stout, J.T., 2003. Retinopathy of prematurity. Pediatr. Clin. North Am. 50 (77–87), vi.

Takao, H., Hayashi, N., Inano, S., Ohtomo, K., 2011. Effect of head size on diffusion tensor imaging. NeuroImage 57, 958–967.

Tournier, J.D., Calamante, F., Connelly, A., 2007. Robust determination of the fibre orientation distribution in diffusion MRI: non-negativity constrained super-resolved spherical deconvolution. NeuroImage 35, 1459–1472.

Tournier, J.D., Calamante, F., Connelly, A., 2012. MRtrix: diffusion tractography in crossing fiber regions. Int. J. Imaging Syst. Technol. 22, 53–66.

Volpe, J.J., 2009. Brain injury in premature infants: a complex amalgam of destructive and developmental disturbances. Lancet Neurol. 8, 110–124.

Vos, S.B., Jones, D.K., Viergever, M.A., Leemans, A., 2011. Partial volume effect as a hidden covariate in DTI analyses. NeuroImage 55, 1566–1576.

Vos, S.B., Jones, D.K., Jeurissen, B., Viergever, M.A., Leemans, A., 2012. The influence of complex white matter architecture on the mean diffusivity in diffusion tensor MRI of the human brain. NeuroImage 59, 2208–2216.

Wasserstein, J., Barr, W.B., Zappulla, R., Rock, D., 2004. Facial closure: interrelationship with facial discrimination, other closure tests, and subjective contour illusions. Neuropsychologia 42, 158–163.

Wechsler, D., 1999. Wechsler Abbreviated Scale of Intelligence (WASI). The Psychological Corporation.

Wheeler-Kingshott, C.A., Cercignani, M., 2009. About "axial" and "radial" diffusivities. Magn. Reson. Med. 61, 1255–1260.

Yeatman, J.D., Dougherty, R.F., Myall, N.J., Wandell, B.A., Feldman, H.M., 2012. Tract profiles of white matter properties: automating fiber-tract quantification. PLoS One 7, e49790.